Double resistive superconducting transition in $Sm_{2-x}Ce_xCuO_{4-y}$

E. A. Early,[*] C. C. Almasan, R. F. Jardim,[†] and M. B. Maple

Department of Physics and Institute for Pure and Applied Physical Sciences,
University of California, San Diego, 9500 Gilman Drive, La Jolla, California 92093

We report a systematic study of the double resistive superconducting transition in carefully prepared polycrystalline samples of the electron-doped superconducting series $Sm_{2-x}Ce_xCuO_{4-y}$ for $0.12 \leq x \leq 0.20$. From high-resolution x-ray-diffraction measurements, the solubility limit of Ce in this series is slightly greater than 0.16. An intrinsic double resistive transition present in all superconducting compounds is attributed to the granularity of these polycrystalline samples. There is a partial transition when the grains become superconducting at a temperature T_{c1}, and coupling between grains at a lower temperature T_{c2} apparently completes the transition. Only the transition associated with coupling between grains is observed in magnetic-susceptibility measurements due to inhomogeneous grains and large penetration depths. From compositional dependences of resistive and magnetic measurements, the superconducting volume fraction increases linearly with increasing dopant concentration up to the solubility limit, while the best coupling between grains is at a dopant concentration of 0.15. Thus, there is a subtle relationship between doping and coupling in this series. Also, arguments for a true thermodynamic phase transition at T_{c2} are given.

I. INTRODUCTION

A significant development in the field of cuprate high-temperature superconductors was the discovery of compounds of the form $R_{2-x}M_xCuO_{4-y}$ (R = Pr, Nd, Sm, or Em; M = Ce or Th; $x \approx 0.15$)[1−4] for which electron, rather than hole, doping is apparently responsible for superconductivity.[5,6] Obviously, comparisons between hole- and electron-doped cuprate superconductors have very important implications for theories of high-temperature superconductivity.

There is significant variety within the family of electron-doped cuprate superconductors, of, for example, their magnetic properties[7] and superconducting transition temperatures. For five of the seven superconducting compounds of the form $R_{1.85}M_{0.15}CuO_{4-y}$, the superconducting transition temperature T_c is close to 20 K, while it is only ≈ 8 K for $Eu_{1.85}Cu_{0.15}CuO_{4-y}$ and ≈ 2 K for $Sm_{1.85}Th_{0.15}CuO_{4-y}$. This variation of T_c with composition is particularly interesting, as it could be useful in determining some of the relevant factors for high-temperature superconductivity. Therefore, it will be important to study the electron-doped compounds with transition temperatures less than 20 K in more detail, particularly their dopant concentration dependences. In order to do this, however, those compounds with $T_c < 20$ K must be compared to a compound with $T_c \approx 20$ K. A logical choice is $Sm_{1.85}Ce_{0.15}CuO_{4-y}$, since $T_c \approx 20$ K for this compound and the two compounds with $T_c < 20$ K can be obtained by appropriate substitutions: either Eu for Sm or Th for Ce.

For this reason, polycrystalline samples in the series $Sm_{2-x}Ce_xCuO_{4-y}$ were investigated initially in anticipation of comparisons with other series, as well as providing an extension of a previous study of the compositional

dependences of electron-doped superconductors.[8] However, a double resistive superconducting transition present in all samples shifted the focus of the research to a consideration of the origin of this feature. Therefore, the results from electrical resistivity and magnetic-susceptibility measurements presented here provide a systematic study of this feature in a series of electron-doped cuprate superconductors as a function of Ce dopant concentration. In addition, x-ray powder-diffraction measurements were used to determine the solubility limit of Ce.

II. SAMPLE PREPARATION AND CHARACTERIZATION

Polycrystalline samples in the series $Sm_{2-x}Ce_xCuO_{4-y}$ for $0.12 \leq x \leq 0.20$ in increments of 0.01 were prepared by a solid-state reaction technique, with the aim of obtaining as stoichiometric and homogeneous samples as possible. The starting materials were 99.99% pure Sm_2O_3, CeO_2, and CuO. To ensure stoichiometry, the first two oxides were heated at 900 °C overnight to remove any absorbed water, and all weighing was performed in an atmosphere of ultra high-purity argon. For each sample, an amount of CeO_2 was weighed first, and amounts of the other two oxides were weighed to within 0.02% of the values calculated from the weight of CeO_2. All three oxides were combined in a glass jar, tumbled to mix, and exposed to air for several hours so that water vapor would be absorbed by Sm_2O_3 to prevent it from adhering to the glass.

The oxides were transferred directly to alumina crucibles and reacted at 900 °C in air for 18 h. This resulted in gray, contracted oxide mixtures, which were ground by hand with an agate mortar and pestle. The mixtures

were not uniform, as unreacted Sm_2O_3 was clearly visible, so they were ground until they were a uniform gray color and for an additional 5 min. The mixtures were reacted at 1000 °C in air for at least 1 d, after which the samples were dark gray and compacted. To obtain improved homogeneity, the samples were ball milled for 1 h with a centrifugal unit using an agate jar and balls. The resulting fine powder was pressed into pellets in a stainless-steel die at a pressure of ~4 kbar. The pellets were returned to the alumina crucibles and sintered in air at 1100 °C for 3 d, after which the furnace was cooled to 900 °C and the pellets were removed to cool in air. The samples were dense and cohesive in nature, dark gray in color, and cylindrical in shape.

A slight reduction of the oxygen content is necessary to make electron-doped cuprates superconducting.[1,5,9] Sample disks were placed upright in a ceramic boat, put into a tube furnace with flowing helium gas, and heated at a constant temperature between 870 and 1000 °C. After 18 h, the disks were cooled to room temperature in 1.5 h. The resistive superconducting transition temperature T_c, here defined as the midpoint of the resistive transition, depends sensitively on the reduction temperature. For the compound $Sm_{1.85}Cu_{0.15}CuO_{4-y}$, T_c varies from 14.3 to 20.7 K after reductions at 870 and 950 °C, respectively. The width of the transition, defined as the temperature difference between the 90 and 10 % resistive drops, is a nearly constant 2.5 K with reduction temperatures up to 950 °C. With higher temperatures, the transition broadens, and the sample begins to decompose at approximately 980 °C. Thus, all samples in the series $Sm_{2-x}Ce_xCuO_{4-y}$ were reduced at 950 °C.

To check for impurity phases and to calculate lattice parameters, high-resolution x-ray powder-diffraction patterns, using Si as an internal standard, were taken on a Rigaku "Rotaflex" RU-200B powder diffractometer with Cu $K\alpha$ radiation. Electrical resistivity measurements were used to gain information about electrical transport properties and the superconducting transition. Four gold contact pads were formed on bar-shaped samples by applying bright brushing gold and curing it at 400 °C for 2 min. Copper electrical leads were attached to these pads using silver epoxy cured at 200 °C for 3 min. The resulting contact resistances were less than 10 Ω. Resistivity as a function of temperature was measured in a ^{4}He cryostat with a Linear Research LR-400 ac resistance bridge operating at a frequency of 16 Hz. The excitation current could be adjusted over several orders of magnitude.

Magnetic-susceptibility measurements, performed on bar-shaped samples using a Quantum Design dc superconducting quantum interference device (SQUID) magnetometer, provided information about the superconducting transition and shielding and volume fractions. To obtain the superconducting volume fraction, the applied magnetic field was less than 5 Oe in order to remain below the lower critical field H_{c1} in these compounds,[10] and the value of the applied field was corrected for the remnant field in the magnet. The procedure during measurement was always to cool the sample to 5 K with no field (zero-field-cooled), apply the field, warm the sample above its superconducting transition temperature, and then cool the sample to 5 K (field-cooled).

III. RESULTS AND DISCUSSION

High-resolution x-ray-diffraction patterns were obtained for most of the samples in the series $Sm_{2-x}Ce_xCuO_{4-y}$. The angles of the 12 prominent peaks for $20° \leq 2\theta \leq 60°$ were corrected with an internal Si standard, and these peaks were indexed from the pattern of Sm_2CuO_4.[11] From these angles and indices, the lattice parameters a_0 and c_0 for each sample were computed for a tetragonal lattice using a least-squares algorithm. The results are shown in Fig. 1, where the ratio c_0/a_0, with its errors, is plotted as a function of Ce dopant concentration x. The ratio of the lattice parameters was chosen because it is not as susceptible to errors as are the individual values. There are clearly two ranges of x in which c_0/a_0 is linear: one for $0.12 \leq x \leq 0.16$ and another for $0.16 \leq x \leq 0.20$. The data in both ranges were fit with straight lines, also shown in Fig. 1, which intersect at a dopant concentration of 0.164.

Small amounts of an impurity phase were detected in samples with Ce concentrations $x \geq 0.17$. This phase was identified as $SmCeO_{3.5}$ for two reasons. One, the compound $NdCeO_{3.5}$ is known to exist, and the angles and relative intensities of the peaks of the impurity phase are very similar to those for this compound.[12] Two, the detection of $SmCeO_{3.5}$ is consistent with a phase diagram of Sm_2O_3, CeO, and CuO with tie lines joining the compounds CuO, $SmCeO_{3.5}$, and $Sm_{2-x}Ce_xCuO_{4-y}$. The inset of Fig. 1 shows the intensity of the (222) $SmCeO_{3.5}$ peak relative to that of the (103) peak of $Sm_{2-x}Ce_xCuO_{4-y}$ plotted as a function of Ce dopant concentration x. A linear fit of this data, also shown in the inset, indicates that the impurity vanishes at a dopant concentration of 0.163.

The remarkably good agreement between the dopant concentrations at which the two linear regions in Fig. 1
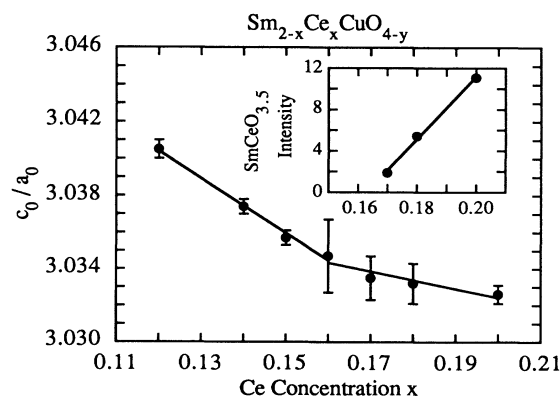

FIG. 1. Ratio of the lattice parameters c_0/a_0, with errors, as a function of Ce dopant concentration x in $Sm_{2-x}Ce_xCuO_{4-y}$. Inset: ratio of $SmCeO_{3.5}$ (222) to $Sm_{2-x}Ce_xCuO_{4-y}$ (103) peak intensities as a function of Ce dopant concentration x. The lines are linear fits to the data.

intersect (0.164) and at which the impurity phase vanishes (0.163) is compelling evidence that the solubility limit of Ce in the series $Sm_{2-x}Ce_xCuO_{4-y}$ is slightly greater than 0.16. In comparison, this is lower than the limit of ≈ 0.20 in $Pr_{2-x}Ce_xCuO_{4-y}$ and $Nd_{2-x}Ce_xCuO_{4-y}$ (Refs. 1, 3, and 8) and the same as the limit in $Eu_{2-x}Ce_xCuO_{4-y}$ (Ref. 13) and $Gd_{2-x}Ce_xCuO_{4-y}$ (Ref. 14). This limit is also lower than the value of ≈ 0.18 found by another group[15] for the same series as studied here, the discrepancy likely being due to differences in the sample preparation techniques between the two groups. The general trend of decreasing Ce dopant solubility with heavier lanthanide element is probably the result of a concomitant decrease in the stability of the crystal structure of these electron-doped cuprates.[16]

Electrical resistivity measurements were performed on all samples of the series $Sm_{2-x}Ce_xCuO_{4-y}$. The results at low temperatures under identical conditions for samples with $0.13 \leq x \leq 0.18$ are shown in Fig. 2, where the normalized electrical resistivity $\rho(T)/\rho_{max}$ for each dopant concentration is plotted as a function of temperature. The inset for $x = 0.15$ shows the normalized electrical resistivity of this sample for all temperatures below room temperature. For compounds with $x \neq 0.15$, the resistive superconducting transition occurs at two different, distinct temperatures. There is a partial transition at a temperature of ≈ 20 K, denoted by T_{c1}, for all dopant concentrations x. The superconducting transition

is not complete, however, until the resistivity decreases again at a lower temperature, that varies with x, denoted by T_{c2}. These two transition temperatures are indicated in Fig. 2 for the sample with $x = 0.16$. This behavior of the resistive superconducting transition is termed a double resistive transition, since it occurs at two transition temperatures, T_{c1} and T_{c2}. For the compound with $x = 0.15$, the two transition temperatures are nearly equal.

From measurements of magnetic susceptibility, presented below, it is clear that the resistive transition at T_{c2} is associated with superconductivity because of a large diamagnetic signal at and below this temperature. The evidence for the transition at T_{c1} also being associated with superconductivity is not as direct, relying instead upon experiments with various reduction temperatures. As discussed above, reduction is necessary for superconductivity in the compound $Sm_{1.85}Ce_{0.15}CuO_{4-y}$, and the transition temperature increases with increasing reduction temperature up to $\sim 970\,^{\circ}C$. The electrical resistivities of samples with $x = 0.16$ and 0.17 were measured after no reduction and after reduction at temperatures of 900 and 950 °C. The values of both T_{c1} and T_{c2} followed the same trend as the transition temperature for the compound with $x = 0.15$; there was no resistive transition for the sample that was not reduced, and both transition temperatures increased with increasing reduction temperature. Thus, the transition at T_{c1} is the result of superconductivity and not, for example, of a structural transition.

Further experiments indicate that the double resistive transition is intrinsic to these samples. The first samples of this series had this feature, which at that time was attributed to large-scale inhomogeneities. This motivated refinement of the preparation technique in order to obtain more homogeneous samples, particularly by ball milling. As Fig. 2 shows, however, this did not result in only one resistive transition. The cooling rate after reduction was varied between two extremes to determine if oxygen ordering was responsible for the double resistive transition. For samples reduced at 950 °C and then either slow cooled to room temperature over a period of 8 h or quenched directly into liquid nitrogen, the resistive transitions occurred at the same two temperatures, thus ruling out this hypothesis. The method in which the leads were attached to the samples was not responsible for the double resistive transition, as leads were also attached without the use of bright brushing gold either by using only a silver conductor composite, which cures at room temperature, or by evaporating gold pads onto the samples and then attaching leads with silver epoxy. In all cases, the double resistive transition was present. In addition, preliminary results from measurements of current-voltage characteristics indicate that the double resistive transition is present in the data. Thus, it is not an artifact of the LR-400 resistance bridge used for the measurement of resistivity.

The conclusion from the experiments with preparation technique, cooling rate, method of lead attachment, and measurement technique is that the double resistive transition observed in the series $Sm_{2-x}Ce_xCuO_{4-y}$ is intrinsic

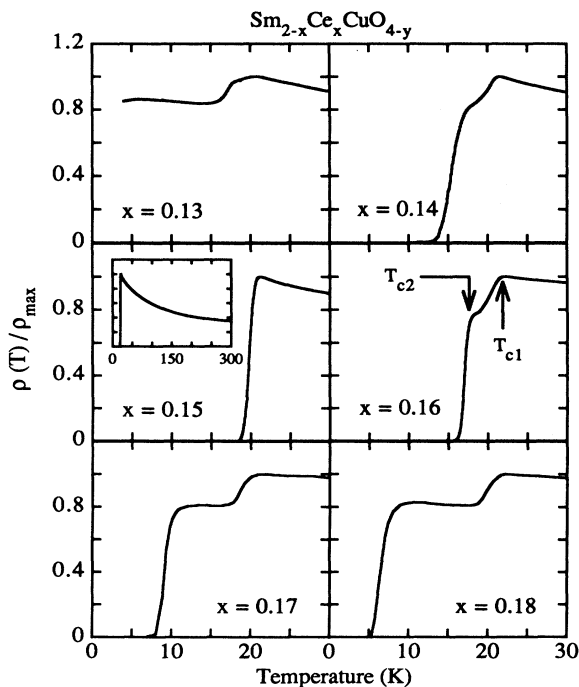FIG. 2. Normalized electrical resistivity $\rho(T)/\rho_{max}$ as a function of temperature of $Sm_{2-x}Ce_xCuO_{4-y}$ for Ce dopant concentrations $0.13 \leq x \leq 0.18$, with two transition temperatures T_{c1} and T_{c2} indicated for $x = 0.16$. Inset for $x = 0.15$: normalized electrical resistivity for temperatures below room temperature.

to these compounds. It persists despite the above-mentioned attempts to eliminate it. There are also examples of double resistive transitions in the literature for $Nd_{1.85}Ce_{0.15}CuO_{4-y}$ (Refs. 17 and 18) and for the series $Nd_{2-x}Ce_xCuO_{4-y}$ (Refs. 19 and 20), which are similar to those shown in Fig. 2. Therefore, this feature is likely a general property of polycrystalline electron-doped superconducting cuprates and not simply of the series $Sm_{2-x}Ce_xCuO_{4-y}$.

Magnetic-susceptibility measurements were performed on samples of the series $Sm_{2-x}Ce_xCuO_{4-y}$ for $0.14 \leq x \leq 0.19$. The results under zero-field-cooled conditions in a field of 1 Oe are shown in Fig. 3, where the superconducting shielding fraction $-4\pi\chi$ is plotted as a function of temperature for dopant concentrations $x = 0.14$, 0.15, and 0.16. Also shown in Fig. 3 are the results from electrical resistivity measurements on the same samples, with normalized electrical resistivity plotted as a function of temperature. There is a relatively abrupt onset of diamagnetism, with its sharpness increasing with increased dopant concentration. Figure 3 was plotted with both magnetic-susceptibility and electrical resistivity data to illustrate an important point; namely, there is no or, at best, very little, diamagnetism at T_{c1}. The magnetic transition occurs instead at T_{c2}. The absence of a magnetic superconducting transition at T_{c1} as measured by the SQUID magnetometer was corroborated by ac susceptibility measurements on these samples.

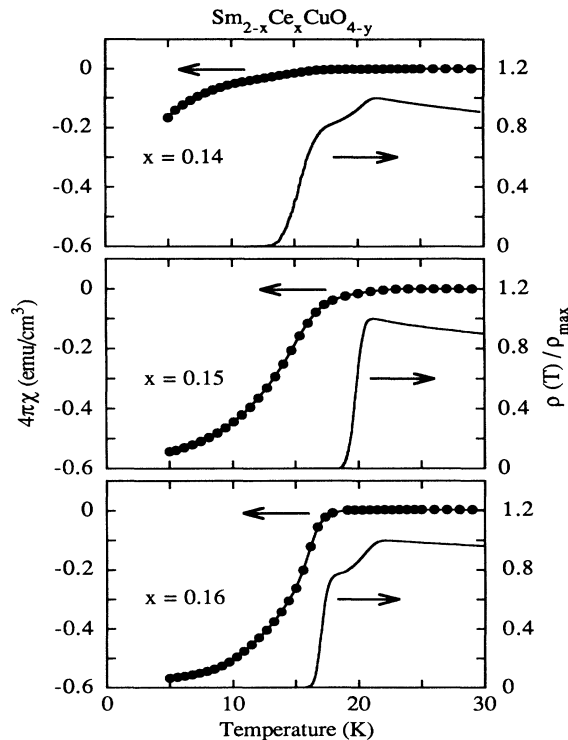The superconducting volume fraction is given by field-cooled results, which for these samples yield approximate superconducting volume fractions of 8, 19, and 30 % for dopant concentrations of 0.14, 0.15, and 0.16, respectively. These are comparable to values obtained in a previous study[8] and indicate that, even with an improved sample preparation technique, the superconducting volume fraction in polycrystalline electron-doped cuprate superconductors is still low.

Since the samples are polycrystalline by virtue of the preparation technique, an understanding of the results presented above must be based upon their granularity. The importance of granularity is demonstrated by its effects on the electrical transport properties of these samples. The inset of Fig. 2 shows that the normal-state resistivity exhibits weakly semiconducting behavior below room temperature. This contrasts with the normal-state behavior for the same temperatures of single crystals of these compounds,[21-23] which is metallic in the range of dopant concentration studied here. This suggests that the grain boundaries of polycrystalline samples are not metallic and determine the nature of the normal-state resistivity of these samples.

In addition, the transport critical current densities of these samples were estimated by varying the excitation current used to measure the electrical resistivity. The results of such an experiment are shown in Fig. 4 for a sample with a dopant concentration of 0.15, where the normalized electrical resistivity $\rho(T)/\rho_{max}$ is plotted as a function of temperature for different excitation currents. The resistive superconducting transition is quite sharp at the lowest excitation current, but increasing the current broadens the transition at temperatures below T_{c2} and eventually suppresses a complete resistive transition. From the dimensions of the sample, a critical current density of only ~ 500 mA/cm^2 at 4.2 K is estimated. Similar behavior of the electrical resistivity with increasing excitation current was observed for the other samples in the series $Sm_{2-x}Ce_xCuO_{4-y}$, but with even lower critical current densities. The transport critical current density is over five orders of magnitude smaller than the intragranular critical current density obtained magnetically for a polycrystalline sample of $Nd_{1.85}Ce_{0.15}CuO_{4-y}$,

FIG. 3. Magnetic superconducting shielding fraction $-4\pi\chi$ (left axis) and normalized electrical resistivity $\rho(T)/\rho_{max}$ (right axis) as a function of temperature of $Sm_{2-x}Ce_xCuO_{4-y}$ for Ce dopant concentrations $0.14 \leq x \leq 0.16$.
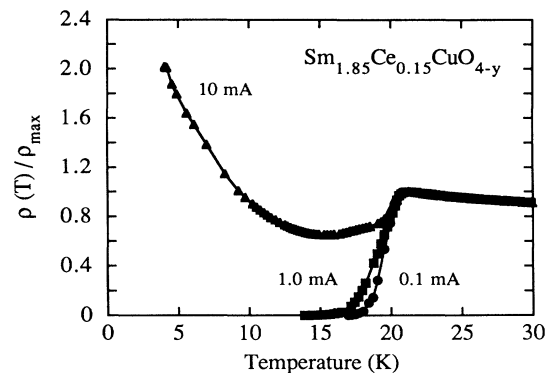

FIG. 4. Normalized electrical resistivity $\rho(T)/\rho_{max}$ as a function of temperature of $Sm_{1.85}Ce_{0.15}CuO_{4-y}$ with excitation currents of 0.1, 1, and 10 mA.

which is greater than 10^5 A/cm^2 at 4.2 K.[7] Thus, the grain boundaries are the limiting factor for the transport critical current density and the grains are weakly coupled.

The granularity of the samples studied here is responsible for the double resistive transition. Qualitatively, the grains have a superconducting transition at T_{c1}, resulting in a partial resistive transition at this temperature. However, Josephson coupling between the grains is weak, so the temperature must be lowered to T_{c2}, where the coupling energy of enough grains is greater than the thermal energy and another resistive transition occurs. Since coupling between grains is more sensitive to the excitation current than is superconductivity within the grains, the resistive transition at T_{c2} broadens much more rapidly with increasing current than does the transition at T_{c1}, as shown in Fig. 4. This behavior is observed for all dopant concentrations. Also, the results presented in Fig. 4 show that the resistive superconducting transition for the sample with $x = 0.15$ is similar to the transitions of samples with other concentrations of Ce. The value of T_{c2} is large enough that the transition is smooth at low excitation currents, but at a current sufficient to suppress a complete transition there is still a decrease in resistivity at T_{c1}, and the relative decrease is nearly identical to that for samples with other Ce concentrations. While the double resistive transition is satisfactorily explained by invoking the concept of granularity and coupling between superconducting grains, the magnetic susceptibility of these samples is puzzling. There should be substantial diamagnetism at T_{c1} when the grains become superconducting. Instead, as shown in Fig. 3, there is no, or very little, diamagnetism at this temperature. There are, however, several factors that can account for the discrepancy between the resistive and magnetic superconducting transitions.

From optical observations of the microstructures of these samples, the grains are relatively large, with an average size of $\sim 5\,\mu$m. Therefore, if the grains are assumed to be homogeneous, attributing the absence of diamagnetism at T_{c1} to the grain sizes being smaller than the London penetration depth is not reasonable. However, there are several reasons to believe that the grains are inhomogeneous. It is well known that the unreactive nature of CeO$_2$ makes it difficult to obtain a uniform distribution of Ce within each grain.[24] One of the purposes of ball milling the samples was to obtain a more homogeneous Ce distribution, but this may not have resulted in complete uniformity. From another study,[25] two processes within each grain are important for superconductivity: the inward diffusion of Ce during sintering and the outward removal of oxygen during reduction. These two processes likely result in a superconducting shell near the surface of each grain, so that even though the grains are fairly large, only a portion is superconducting. This also helps explain the low superconducting volume fractions of these samples.

In addition to inhomogeneities within the grains, large magnetic penetration depths are also important. The London penetration depth λ in Sm$_{1.85}$Ce$_{0.15}$CuO$_{4-y}$ is

fairly large, being close to 1 μm at zero temperature.[10] When this penetration depth is comparable to or larger than the grain size, or the portion of the grain that is superconducting, the diamagnetic susceptibility is greatly reduced from its maximum value. Also, in granular systems the Josephson penetration depth λ_J is an important variable.[26] The Josephson penetration depth is a measure of how far a magnetic field penetrates a Josephson junction, and is typically several orders of magnitude greater than the London penetration depth. In the compound studied here, λ_J should be especially large because it is proportional to $(J_c)^{-1/2}$, where J_c is the critical current density of the junction,[27] and, from above, J_c is very low in these compounds. A large λ_J, comparable to the size of the entire sample, will significantly reduce the diamagnetic susceptibility from its maximum value.[26] Finally, the small value of the lower critical field H_{c1} in these compounds, ~ 1.5 mT at zero temperature,[10] could contribute to a reduced diamagnetic susceptibility.

From the previous discussion, there are several factors that could contribute to the absence of diamagnetic susceptibility at T_{c1}, mainly inhomogeneities within the grains in combination with large London and Josephson penetration depths. At T_{c2}, however, the grains become connected and ordering occurs over a much longer range, resulting in less suppression of the diamagnetic susceptibility by the large penetration depths, primarily λ. Thus, it is at this long-range ordering temperature T_{c2} that there is significant diamagnetism. The breadth of the diamagnetic transition indicates there is a distribution of temperatures at which coupling occurs. At T_{c2} enough grains are coupled to result in a connected path with zero resistance, with additional couplings occurring below this temperature. Also, for all dopant concentrations, the absolute value of the magnetic susceptibility increases with decreasing temperature. This may indicate that, as the temperature is lowered, an increasing number of finite clusters of superconducting grains join the percolative supercluster. This is due to an increase in the coherence between the phases of the superconducting order parameters of the clusters, produced by improved coupling at lower temperatures.

The compositional dependences of the series Sm$_{2-x}$Ce$_x$CuO$_{4-y}$ supply additional information, as well as serving as a basis for comparison with similar dependences in other series of electron-doped cuprates. These compositional dependences are shown in Fig. 5, where (a) $-4\pi\chi$ at 5 K under both field-cooled (FC) and zero-field-cooled (ZFC) conditions, (b) the ratio of maximum resistivity to room temperature resistivity ρ_{max}/ρ_{300}, (c) the resistive superconducting transition temperature T_{c2}, and (d) the ratio of zero-field-cooled to field-cooled values of $-4\pi\chi$ are plotted as a function of Ce dopant concentration x. As discussed below, the first two are associated with properties of the grains, while the second two are associated with coupling between grains.

Since granularity appears to be responsible for the double resistive transition, it is useful to separate the effects of coupling between grains from the properties of the grains. An important property of the grains is their su-
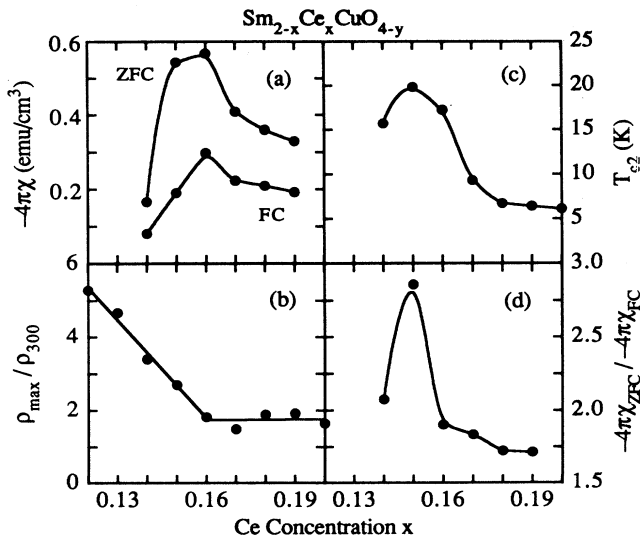
FIG. 5. (a) $-4\pi\chi$ at 5 K under both field-cooled (FC) and zero-field-cooled (ZFC) conditions, (b) the ratio of maximum resistivity to room temperature resistivity ρ_{max}/ρ_{300}, (c) the resistive superconducting transition temperature T_{c2}, and (d) the ratio of zero-field-cooled to field-cooled values of $-4\pi\chi$ as a function of Ce-dopant concentration x in $Sm_{2-x}Ce_xCuO_{4-y}$. The lines in (a), (c), and (d) are guides to the eye and in (b) are linear fits to the data for the two region $x \leq 0.16$ and $x \geq 0.16$.

perconducting volume fraction, given by $-4\pi\chi$ under field-cooled conditions. From Fig. 5 (a), this value increases linearly with increasing Ce dopant concentration up to the solubility limit of 0.16, indicating that either the fraction of superconducting grains or the superconducting portion of each grain is increasing. The latter possibility is more likely if superconductivity is confined to a shell within each grain. For dopant concentrations above the solubility limit, the fraction or portion of superconducting grains remains relatively constant, while effects from impurity phases could cause the slow decrease in $-4\pi\chi$ with increasing x. The resistive transition temperature T_{c1} should also provide information about the grains. From the data shown in Fig. 2, T_{c1} is nearly constant as a function of x, but details are not consistent between different samples of the same composition. For some samples there is a maximum in T_{c1} at $x = 0.15$, while for others there is not, although in almost every case the resistive transition at T_{c1} is sharpest for $x = 0.15$. In addition, the relative drop in resistivity at T_{c1} increases slightly with increasing dopant concentration for $0.13 \leq x \leq 0.16$ and remains constant for $x > 0.16$. This is consistent with an increasing superconducting fraction in the former range of dopant concentrations, since more of the conducting path is superconducting with increasing x and thus the relative decrease in resistivity at T_{c1} also increases.

Two experimental values which are directly proportional to the strength of the coupling between grains are plotted in Figs. 5(c) and 5(d). The second resistive transi-

tion temperature T_{c2} indicates the strength of the coupling, since the higher the transition temperature the greater the coupling energy. The other value is the ratio between the zero-field-cooled and field-cooled values of $-4\pi\chi$. When magnetic-susceptibility measurements were performed on the same sample in both bar and powder forms, the difference between the susceptibilities under both cooling conditions for the bar was nearly absent for the powder, indicating that coupling between grains is responsible for the difference. The curves in Figs. 5(c) and 5(d) are nearly identical, with a definite maximum for $x = 0.15$. Thus, the maximum coupling strength between grains occurs at this dopant concentration.

Finally, returning to the properties of the grains, the ratio of the resistivities ρ_{max}/ρ_{300} correlates with the normal-state resistivity of the sample—the greater the ratio, the more semiconducting the resistivity—and is preferable to the absolute resistivity because of uncertainties in the geometry. From Fig. 5(b), this ratio decreases significantly with increasing Ce dopant concentration up to the solubility limit, by more than a factor of two from $x = 0.12$ to 0.16, and is constant for greater dopant concentrations. This trend is similar to the increasingly metallic behavior in single crystals in the same range of dopant concentrations,[23] and corroborates the dopant solubility limit of slightly greater than 0.16 deduced from x-ray-diffraction measurements. The trend is definitely not due to coupling between grains for the following two reasons. From the data shown in Figs. 5(c) and 5(d), the coupling is optimized for $x = 0.15$, but the minimum in ρ_{max}/ρ_{300} occurs at $x = 0.16$. Also, even though the coupling strength decreases for dopant concentrations greater than the solubility limit, the ratio of the resistivities remains constant.

Summarizing the compositional dependences presented in Fig. 5, there is a smooth change in the properties of the grains with increasing dopant concentration up to the solubility limit, with the superconducting fraction increasing and the grains becoming more metallic. On the other hand, the coupling strength between grains is definitely optimized for $x = 0.15$, since both T_{c2} and $-4\pi\chi_{ZFC}/-4\pi\chi_{FC}$ are a maximum at this dopant concentration. Thus, there is a subtle and complex relationship among the dopant concentration and the strength of the coupling between grains, which will be a challenge for any complete explanation of the properties of polycrystalline electron-doped cuprates.

As in the previous study,[8] the samples studied here have a maximum transition temperature, from both resistive and magnetic measurements, for a Ce dopant concentration $x = 0.15$. However, in the previous study, the superconducting volume fraction was likewise a maximum for this dopant concentration, while in this study the fraction increases with increasing dopant concentration up to the solubility limit. This difference is probably due to the different sample preparation techniques employed in the two studies, with the technique used here believed to be better.

The results discussed above suggest the possibility of phase separation at $x = 0.15$ in the series studied here, as

has been claimed in the series $Nd_{2-x}Ce_xCuO_{4-y}$.[28,29] There, the phase separation was argued to be a nonequilibrium process, which resulted in a sharp peak in $-4\pi\chi$ at a dopant concentration of ≈ 0.16. If phase separation is present in the series $Sm_{2-x}Ce_xCuO_{4-y}$ for $x = 0.15$, a peak would likewise be expected in $-4\pi\chi$ at this dopant concentration, but instead $-4\pi\chi$ increases smoothly up to a dopant concentration of 0.16, as shown in Fig. 5(a). In addition, the relative drop in resistivity at T_{c1}, if due to phase separation, should be greatest at $x = 0.15$ but instead increases slowly with increasing x. Thus, there is no evidence for phase separation in the series $Sm_{2-x}Ce_xCuO_{4-y}$ from the results presented here. However, no definitive conclusion regarding the Ce dopant concentration of the superconducting phase can be reached from the experimental results. Two likely possibilities are that the phase has the starting stoichiometry of the sample or that all samples have the same superconducting phase with, for example, $x = 0.16$. The first possibility implies that all superconducting phases in the series $Sm_{2-x}Ce_xCuO_{4-y}$ have the same transition temperature, while the second is plausible because the superconducting volume fraction increases with increasing dopant concentration to $x = 0.16$. In either case, the stoichiometry of the superconducting phase does not change the conclusions from above that the resistive transition at T_{c2} results from coupling between superconducting grains or that the optimal coupling is achieved for $x = 0.15$.

The experimental results and theoretical analysis of Gerber et al.[30,31] also need to be addressed. They found a double resistive transition in polycrystalline electron-doped cuprates under applied magnetic fields, and attributed this to coupling between grains. In their analysis, this coupling involves a combination of quasiparticle and Josephson tunneling between isolated superconducting grains. However, the experimental results presented here do not support the explanation that the resistivity in the temperature region between T_{c1} and T_{c2} is caused by quasiparticle tunneling. If this type of tunneling is present, the resistivity should increase rapidly with decreasing temperature because the tunneling is a thermally activated process. From the resistivity data presented in Fig. 2, the resistivity in the temperature region between T_{c1} and T_{c2} for all samples is nearly constant. Therefore, quasiparticle tunneling is not significant, and instead it is more likely that there is a competition between the normal-state resistivity and Josephson coupling between the grains. An additional criticism of the model of Gerber et al. is their conclusion that the onset of superconductivity is at a temperature greater than T_{c1}. This is based upon a decrease in resistivity at a temperature above T_{c1} when a magnetic field is applied. However, a negative magnetoresistance was found in measurements performed on nonsuperconducting thin films[32] and single crystals[33] of electron-doped cuprates, indicating that the reduction in resistivity under an applied magnetic field is caused by weak localization of the charge carriers in two dimensions and not by superconductivity.

While a definitive theoretical model of the double resis-

tive transition observed in this series is not available at this time, there are some preliminary conclusions about two possible models for the transition at T_{c2}. One model involves percolation ideas, as illustrated by Deutscher and Rappaport in their study of $Al_{1-x}Ge_x$ films for $0.65 < x < 0.74$.[34] This system is well described by a combination of metallic Al grains embedded in an insulating Ge matrix. If the metallic concentration is below the percolation threshold, an incomplete transition at T_{c1}, followed by a transition at T_{c2}, should be observed. The metallic grains have a superconducting transition at T_{c1} and Josephson tunneling between grains forms a connected superconducting path across the entire sample at T_{c2}. Deutscher and Rappaport observed a reasonable $\sim 70\%$ drop in resistivity at T_{c1} and a concave upward transition, the so-called tail feature, as the zero resistance state was approached. Their results suggested that the transition at T_{c1} also includes a significant number of strongly coupled grains and that the zero resistance state is achieved when more junctions become superconducting when the temperature is lowered.

It is reasonable to consider a percolation model for the experimental results because the superconducting volume fraction, from Fig. 5(a), is always less than the percolation volume threshold of $\sim 30\%$.[35,36] The actual value of the percolation threshold for the samples studied here is complicated by a lack of knowledge about the coordination number of the grains, and is probably greater than 30% due to the asymmetry between the shapes of the conducting grains and the nonconducting grain boundaries. In any event, the results presented here show quite different qualitative and quantitative behaviors from those of Ref. 34. First, the relative drop in resistivity at T_{c1} is nearly independent of Ce concentration, suggesting that there is not a significant distribution of Josephson coupling energies at T_{c1}. This is corroborated by the well-defined plateau in resistivity at temperatures between T_{c1} and T_{c2}, which is not the expected behavior for a system where the number of coupled grains increases with decreasing temperature. The plateau in the resistivity of the series studied here is more typical of the classical behavior of a high-resistance composite where one component has zero resistance. Second, the resistive transition at T_{c2} is abrupt and is concave downward, whereas in percolation systems the transition is broad and concave upward.

The basis for the other theoretical model, and the one that was implicitly followed in the discussions of the experimental results, is that there is a true long-range thermodynamic phase transition at T_{c2}, as described by Deutscher, Imry, and Gunther[37] and Patton, Lamb, and Stroud.[38] Both models start with metallic grains separated by insulating regions, which is similar to the polycrystalline samples studied here. At T_{c1}, a large number of metallic grains become superconducting and the resistivity decreases. At a lower temperatures T_{c2} the phases of the order parameters of the individual grains become coherent and a zero-resistance state is achieved. This transition is, in fact, a true thermodynamic transition of the system with broken phase symmetry and so simple

percolation ideas are not valid. Qualitatively, the decrease in the resistivity at T_{c1} is proportional to the number of superconducting grains and increases significantly when the number is close to the percolation threshold. Below T_{c1}, the resistivity has a well-defined plateau and a thermodynamic phase transition occurs at T_{c2}, with a concave downward resistivity curve.

While the experimental results suggest that a long-range thermodynamic phase transition occurs at T_{c2}, there are several details which need to be clarified. The relative drop in resistivity at T_{c1} is nearly constant for $0.13 \leq x \leq 0.20$, which implies that the superconducting fraction is nearly constant in this concentration interval. This appears to contradict the results obtained from magnetization measurements, as shown in Fig. 5(a), but can be explained if it is assumed that the diamagnetic signal at 5 K also involves a reasonable contribution from coupling between grains. Magnetization measurements at very low fields should be able to resolve such a contribution. Although there are a few discrepancies between the results presented here and the predictions of both theoretical models described above, the qualitative behavior of these materials can best be understood if a true thermodynamic phase transition at T_{c2} is assumed. In marked contrast with hole-doped superconductors, the properties of electron-doped superconductors show clear evidence of an intergranular contribution, which must be taken into account in order to understand the magnetic and transport properties of these materials.[39]

IV. CONCLUSIONS

The results from x-ray powder-diffraction measurements, in conjunction with the compositional dependences of $-4\pi\chi$ and ρ_{max}/ρ_{300}, conclusively determined that the solubility limit of Ce in the series $Sm_{2-x}Ce_xCuO_{4-y}$ is slightly greater than 0.16. The pronounced granularity of these polycrystalline samples, probably due to the unreactive nature of CeO_2, results in a very low transport critical current density and has a significant effect on their resistive and magnetic properties. It causes a double resistive transition where the grains have a superconducting transition at T_{c1}, with a partial decrease in resistivity, while coupling between the grains, and the completed transition, occurs at a lower temperature T_{c2}. However, no diamagnetism is detected at T_{c1}, primarily because the grains are inhomogeneous and the London and Josephson penetration depths are large. Compositional dependences in the series indicate a puzzling result. While the coupling strength between grains is greatest for a dopant concentration $x = 0.15$, the superconducting volume fraction increases with increasing x to the solubility limit. Thus, there is a complex relationship between doping concentration, coupling strength, and superconducting volume fraction. Finally, the results indicate that the transition at T_{c2} is probably due to a true thermodynamic phase transition.

*Present address: National Institute of Standards and Technology, Rm B-258, Bldg 220, Gaithersburg, MD 20899.

†Permanent address: Instituto de Física, Universidade de São Paulo, CP 20516, São Paulo, Brazil.

[1] Y. Tokura, H. Takagi, and S. Uchida, Nature (London), 337, 345 (1989).

[2] J. T. Markert and M. B. Maple, Solid State Commun. 70, 145 (1989).

[3] J. T. Markert, E. A. Early, T. Bjørnholm, S. Ghamaty, B. W. Lee, J. J. Neumeier, R. D. Price, C. L. Seaman, and M. B. Maple, Physica C 158, 178 (1989).

[4] E. A. Early, N. Y. Ayoub, J. Beille, J. T. Markert, and M. B. Maple, Physica C 160, 320 (1989).

[5] H. Takagi, S. Uchida, and Y. Tokura, Phys. Rev. Lett. 62, 1197 (1989).

[6] J. M. Tranquada, S. M. Heald, A. R. Moodenbaugh, G. Liang, and M. Croft, Nature (London) 337, 720 (1989).

[7] C. L. Seaman, N. Y. Ayoub, T. Bjørnholm, E. A. Early, S. Ghamaty, B. W. Lee, J. T. Markert, J. J. Neumeier, P. K. Tsai, and M. B. Maple, Physica C 159, 391 (1989).

[8] N. Y. Ayoub, J. T. Markert, E. A. Early, C. L. Seaman, L. M. Paulius, and M. B. Maple, Physica C 165, 469 (1990).

[9] J. T. Markert, N. Y. Ayoub, T. Bjørnholm, E. A. Early, C. L. Seaman, P. K. Tsai, and M. B. Maple, Physica C 162-164, 957 (1989).

[10] C. C. Almasan, S. H. Han, E. A. Early, B. W. Lee, C. L. Seaman, and M. B. Maple, Phys. Rev. B 45, 1056 (1992).

[11] Pattern 24-998, Powder Diffraction File of the Joint Committee on Powder Diffraction Data (International Center for Diffraction Data, Swarthmore, PA).

[12] Pattern 28-266, Powder Diffraction File of the Joint Committee on Powder Diffraction Data (International Center for Diffraction Data, Swarthmore, PA).

[13] H. Itoh and M. Kusuhashi, Physica C 185-189, 919 (1991).

[14] A. Butera, A. Caneiro, M. T. Causa, L. B. Steren, R. Zysler, M. Tovar, and S. B. Oseroff, Physica C 160, 341 (1989).

[15] M. Klauda, J. P. Ströbel, M. Lippert, G. Saemann-Ischenko, W. Gerhäuser, and H.-W. Neumüller, Physica C 165, 251 (1990).

[16] Y. Y. Xue, P. H. Hor, R. L. Meng, Y. K. Tao, Y. Y. Sun, Z. J. Huang, L. Gao, and C. W. Chu, Physica C 165, 357 (1990).

[17] T. Ekino and J. Akimitsu, Phys. Rev. B 40, 7364 (1989).

[18] A. Krol, C. S. Lin, Z. H. Ming, C. J. Sher, Y. H. Kao, C. L. Lin, S. L. Qui, J. Chen, J. M. Tranquada, M. Strongin, G. C. Smith, Y. K. Tao, R. L. Meng, P. H. Hor, C. W. Chu, G. Cao, and J. E. Crow, Phys. Rev. B 42, 4763 (1990).

[19] V. Garcia-Vazquez, S. Mazumdar, C. M. Falco, C. Barlingay, and S. H. Risbud, in Electron-Phonon Interaction in Oxide Superconductors, Proceedings of the First CINVESTAV Superconductivity Symposium, edited by R. Baquero (World

Scientific, Singapore, 1991).

[20] J. W. Chen and W. C. Chou, Physica C **172**, 229 (1990).

[21] Y. Hidaka and M. Suzuki, Nature (London) **338**, 635 (1989).

[22] Y. Dalichaouch, B. W. Lee, C. L. Seaman, J. T. Markert, and M. B. Maple, Phys. Rev. Lett. **64**, 599 (1990).

[23] S. J. Hagen, J. L. Peng, Z. Y. Li, and R. L. Greene, Phys. Rev. B **43**, 13 606 (1991).

[24] M. E. López-Morales, R. J. Savoy, and P. M. Grant, Solid State Commun. **171**, 1077 (1989).

[25] R. F. Jardim, E. A. Early, and M. B. Maple (unpublished).

[26] J. R. Clem, Physica C **153-155**, 50 (1988).

[27] B. D. Josephson, Adv. Phys. **14**, 419 (1965).

[28] P. Lightfoot, D. R. Richards, B. Dabrowski, D. G. Hinks, S. Pei, D. T. Marx, A. W. Mitchell, Y. Zheng, and J. D. Jorgensen, Physica C **168**, 627 (1990).

[29] J. D. Jorgensen, P. Lightfoot, S. Pei, B. Dabrowski, D. R. Richards, and D. G. Hinks, in *Advances in Superconductivity III*, Proceedings of the 3rd International Symposium on Superconductivity, edited by K. Kajimura and H. Hayakawa (Springer-Verlag, Tokyo, 1991).

[30] A. Gerber, T. Grenet, M. Cyrot, and J. Beille, Phys. Rev. Lett. **65**, 3201 (1990).

[31] A. Gerber, T. Grenet, M. Cyrot, and J. Beille, Phys. Rev. B **43**, 12 935 (1991).

[32] A. Kussmaul, J. S. Moodera, P. M. Tedrow, and A. Gupta, Physica C **177**, 415 (1991).

[33] S. J. Hagen, X. Q. Xu, Jiang, J. L. Peng, Z. Y. Li, and R. L. Greene, Phys. Rev. B **45**, 515 (1992).

[34] G. Deutscher and M. L. Rappaport, J. Phys. (Paris) Colloq. **39**, C6-581 (1978).

[35] V. K. S. Shante and S. Kirkpatrick, Adv. Phys. **20**, 325 (1971).

[36] S. Kirkpatrick, Rev. Mod. Phys. **45**, 574 (1973).

[37] G. Deutscher, Y. Imry, and L. Gunther, Phys. Rev. B **10**, 4598 (1974).

[38] B. R. Patton, W. Lamb, and D. Stroud, in *Inhomogeneous Superconductors—1979*, Proceedings of the Conference on Inhomogeneous Superconductors, AIP Conf. edited by T. L. Francavilla, D. U. Gubser, J. R. Leibowitz, and S. A. Wolf Proc. No. 58, (AIP, New York, 1980), p. 13.

[39] A. Gerber, Th. Grenet, M. Cyrot, and J. Beille, Phys. Rev. B **45**, 5099 (1992).